Bayesian derivation of electron temperature profile using JET ECE diagnostics

S. Schmuck[1], J. Svensson[1], E. de la Luna[2], L. Figini[3], T. Johnson[4], B. Alper[5], M. Beurskens[5], J. Fessey[5], T. Gerbaud[6], A. Sirinelli[5] and JET EFDA Contributors*

JET-EFDA, Culham Science Centre, Abingdon, OX14 3DB, UK

[1]Max-Planck-Institut für Plasmaphysik, Teilinstitut Greifswald, EURATOM-Assoziation, D-17491 Greifswald, Germany

[2] Laboratorio Nacional de Fusion, Asociacion EURATOM-CIEMAT, Madrid, Spain

[3] Istituto di Fisica del Plasma, CNR, Euratom-ENEA-CNR Association, Milano, Italy

[4]Association EURATOM-VR, Fusion Plasma Physics, EES, KTH, SE-10044 Stockholm, Sweden

[5]Euratom/CCFE Fusion Association, Culham Science Centre, Abingdon, Oxon, OX14 3DB, UK

[6]FOM Institute for Plasma Physics Rijnhuizen, Association EURATOM-FOM, Trilateral Euregio Cluster, The Netherlands

1. Introduction

For plasmas in fusion devices using magnetic field confinement electron cyclotron emission (ECE) is inherent. Thereby, plasma electrons emit an intensity spectrum at the gyration frequency and its harmonics for each polarisation state. For a broad plasma parameter range the plasma is optically thick and acts therefore like a blackbody in the main spectral part of the 2nd harmonic in X-mode polarisation. By utilization of the Rayleigh-Jeans law the electron temperature profile can be determined from the intensities measured by individual spectral channels and the magnetic field along the diagnostic line of sight. At the tokamak JET the described technique is routinely applied in the spectral range 100-200GHz measured by the absolute calibrated Michelson interferometer. For the ECE spectrum in the spectral range of the 4th and 5th harmonic, also covered by the Michelson interferometer at JET, the plasma has become optically thin and thus the blackbody model is not valid anymore. As consequence, the optically thin ranges are influenced by the electron density and each of the spectral channels affected gives separate information about the density profile integrated along the line of sight. Thus, information about the temperature and density profiles can be extracted from the extended spectral range by an improved analysis. Furthermore, by the use of several harmonics probing different regions in the velocity phase space the determined temperature gives an improved ensemble average. For an improved analysis a model predicting the ECE spectrum for given electron temperature and density profile and magnetic field is mandatory. Since the ECE theory is well understood and ECE ray-tracing codes like SPECE have been developed [5] such a model is available. At JET a first order analysis of the optically thin and thick spectral ranges has been achieved already by manual manipulation of the plasma parameters fed to SPECE [6,7]. To treat the complex inference problem more consistently, a model for the Michelson interferometer has been implemented together with the absolute calibration into the Minerva Bayesian inference framework [3], previously used for modelling of other JET diagnostics [8,9,10,11] and different equilibrium inference studies [12,13,14].
The novel Bayesian technique removes the need for window functions, zero-padding and phase correction associated with Fourier transformation based techniques for the analysis of interferogram data [15]. But the diagnostic model needs to take into account dispersion inside the interferometer itself. The proof of principle for the new approach, as described below, shows the feasibility for the inference of the T_e and n_e profiles and a 1st order correction of the vacuum toroidal magnetic field independent on other diagnostics.

2. Framework Minerva

The Bayesian probability theory treats uncertain knowledge or information which is inherent in the field of data analysis. Thereby, the knowledge about model parameters, like physics quantities, is encoded in the prior and posterior distribution stating the information before and after the analysis for a used model. A Bayesian graphical model [3] links model parameters and measured data by describing the functional and probabilistic dependencies, completely.

Such graphical models can be constructed by the framework Minerva. In addition, Minerva provides the tools to analyse graphical models: optimization methods find the maximum posterior (MAP) which is the most plausible model parameter vector and uncertainties for the model parameter can be computed easily even for asymmetric posterior distributions.

3. Model for ECE Spectrum

For given plasma parameters the model used to predict the ECE spectrum is realized by the ECE ray-tracing code SPECE, which is coupled to Minerva via a web service. SPECE solves the dispersion relation, using the fully relativistic formulation for the computation of the dielectric tensor elements. In order to get reliable results for the spectral range up to the 5th harmonic with SPECE the dielectric tensor is computed with a series expansion in the Larmor radius up to the 5th order. The spectra of different polarization states are mixed dependent on the line of sight, the orientation of the diagnostic in-vessel antenna and the magnetic field configuration. Since the plasma is optically thin for certain spectral ranges, like the 4th and 5th harmonic, wall properties like reflectivity and mode scrambling are considered by SPECE. However, the corresponding nominal coefficients are set to R_R=0.55 and R_{MS}=0.38 determined empirically [6]. To evaluate a spectrum SPECE needs quantities like the poloidal flux ψ (or normalized ψ_N) as a function of major radius R and height Z, and the poloidal current function f_{POL} and the vacuum toroidal magnetic field B_{TOR} at centre of the vessel. The density and temperature profiles need to be given in terms of normalized flux ψ_N. In principle, SPECE takes the finite antenna pattern of the diagnostic into account. For the Michelson interferometer at JET the antenna pattern is approximated by the central ray of the line of sight.

4. Model for Michelson Interferometer

The basic concept of a Michelson interferometer is described by the interference pattern or interferogram as seen by the detector dependent on the optical path difference for the beams propagating in each of the two diagnostic arms. Therefore, the diagnostic measures the spectrum of a source indirectly. In the field of Fourier transform spectroscopy the spectrum is recovered from the interferogram by standard techniques using window functions, zero-padding, cosine and sine transformation and phase correction. Window functions are applied to reduce leakage in the spectral domain due to the finite data set. Zero-padding increases the frequency resolution artificially and ensures the utilization of fast Fourier transform methods. By phase correction the influence of the interferogram asymmetry is reduced. The diagnostic model implemented in Minerva goes without window functions since all non-vanishing spectral components are taken into account, zero-padding, sine transformation and phase correction. The model is expressed by the integral in the spectral domain

$$V(x) = \frac{1}{2}\int_0^\infty I_f C_f A\left(1+\cos\left(2\pi\frac{f}{c}x+\alpha_f\right)\right)df \,, \qquad (1)$$

whereat the measured interferogram V (in terms of Volts) as a function of the optical path difference x, the spectrum I_f for the source in front of the interferometer input port, the calibration factors C_f, the post-detection amplification A and the dispersion α_f enter. Quantities in (1) subscribed with f are dependent on frequency. Usually, measured interferograms, like in [1], show asymmetries which are expected to be caused by dispersion on the diagnostic side. Theoretically, dispersion arises in optical components and beam splitters with varying refractive index, in the detector electronic circuit, due to mirror misalignment and/or other effects. Since the presented model includes the dispersion inside the diagnostic itself, (1) generalizes the standard text book model with vanishing α_f. As a consequence, the separation of effects caused by the diagnostic and the actual source to be investigated becomes possible. On the contrary, the phase correction of the standard analysis convolutes features of the diagnostic and the input spectrum emitted by the source. Due to the discretization by the data acquisition, triggered by the spatial increment $\Delta x=80\text{x}10^{-6}$m for

the position of the moving mirror in the interferometer, the grid of the optical path difference is given by $x=x_i=i(2\Delta x)+x_0$. Thereby, x_0 describes the shift from the recorded maximum voltage at the zero-path-difference position with index i_{ZPD} to the continuous one and is evaluated by a quadratic fit to V_{iZPD-1}, V_{iZPD} and V_{iZPD+1}. Following the standard analysis, the maximum inferable frequency is 936.85 GHz and the spectral resolution is set to 5.68GHz. The absolute calibration of the Michelson interferometer carried out in 2010 has been analysed with Minerva to get C_f in (1) with uncertainties. Thereby, the diagnostic shows to be sensitive at least in the spectral range 68-520GHz.

5. Inference of Plasma Parameters

In principle, the ECE spectrum $I_f(T_e,n_e,B)$ predicted by SPECE at individual frequencies enters the diagnostic model described by equation (1). But, practically, the finite spectral channel bandwidth (5.68GHz) needs to be modelled by having 5 sub channels equally distributed per channel. The corresponding intensities are averaged to give the intensity measured by the spectral channel. So far, the functional dependence between T_e, n_e and magnetic field B and interferogram data is finalized. Interferogram data is analysed for the JET pulse 79853, t=14.72s. But in order to save computing resources the analysis is performed in two steps. In the first step for given calibration C_f with uncertainties, I_f and α_f are inferred for broad Gaussian priors in the spectral range up to 500GHz. For the second step the focus lies on the spectral range 68-363GHz which is predicted by SPECE for given plasma parameters T_e, n_e and B_{TOR} using equilibrium quantities of the standard EFIT output for $\psi_N(R,Z)$ and f_{POL}. Thereby, the flux surfaces remain spatially fixed. The profiles are assumed to be constant on flux surface and therefore are inferred in terms of ψ_N. For the temperature and density the range is $\psi_N=[0,1]$ with increment $\Delta\psi_N=0.05$. Besides the profiles B_{TOR} is inferred. In total the analysis has 44 model parameters described by a multivariate Gaussian prior. The prior mean for B_{TOR} equals 2.4547T provided by EFIT and the standard deviation is chosen broad with 0.1T. For the profiles the prior means are set to 0.1keV and $0.1\text{x}10^{19}\text{m}^{-3}$, respectively. Thus, no other profile diagnostic is involved. The non-vanishing elements of the variance matrix, entering the prior for the profile parameters, are chosen large to suppress their influence. Nevertheless, off-diagonal elements are chosen such that the scale length, for which changes occur, is $\Delta\psi_N=0.2$. To find the maximum posterior (MAP) for the plasma parameters, Minerva optimization routines are used. At the MAP B_{TOR} is increased by 2.1%. Since the flux surfaces are spatially fixed, the only degree of freedom to change anything else but the profiles is B_{TOR}. Therefore, the gained magnetic field correction of ~2% includes not only the magnetic field calibration adjustment but other incorrect model assumptions. One example is that, the standard EFIT analysis, from which quantities have been used here, is constraint just by magnetic diagnostics. The inferred T_e profile has the central temperature of 7.7 keV, falls monotonously neglecting a slightly hollow region around $\psi_N=0.6$ and vanishes almost at $\psi_N=1.0$ (see Fig. 1a). The derived T_e profile is similar below $\psi_N=0.8$ compared with the profile obtained with the standard technique from the 2nd harmonic X-mode range. The latter shows a discrepancy between low and the high field side, likely to be caused by erroneous mapping, i.e. the localisation of the flux surfaces, related to EFIT. In addition, the fact, that the inferred T_e profile is enclosed by the standard T_e profile in the plasma centre ($\psi_N<0.3$), points again to mapping problems caused by EFIT. The inferred profile drops and vanishes around the closed flux surface not deduced by the standard technique. Caused by the low frequency resolution, the determined pedestal is not as steep as the one measured by the high resolution Thomson scattering diagnostic (HRTS) at JET (not shown). The oscillating behaviour and the reduction by 30-50% of the derived density profile (see Fig. 1b), compared with results of other density diagnostics like the reflectometer (not shown) and HRTS are obvious. The discrepancy can be caused by two model

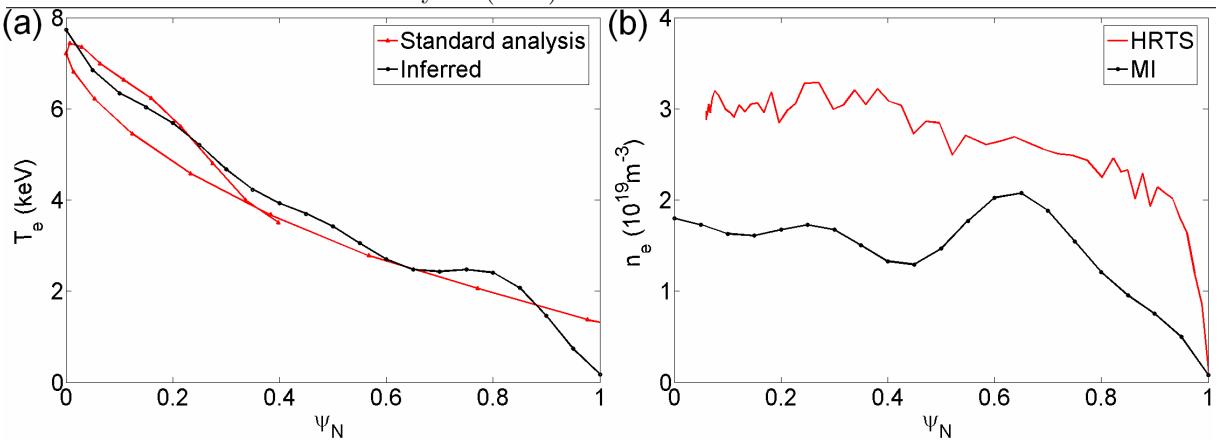

Fig. 1. Derived profiles (black) for Michelson interferometer in terms of normalized flux ψ_N for JET pulse 79853, t=14.72s. (a) Temperature T_e. The standard analysis (red) does not assume T_e preservation on flux surfaces. (b) Density n_e. The inferred density is smaller with respect to the one (red) measured by the high resolution Thomson scattering (HRTS) diagnostic and others.

assumptions made but not checked. Firstly, the wall property coefficients R_R and R_{MS} empirically determined are overestimated which would decrease the density everywhere. Secondly, since channels in the optically thin range measure line-integrated intensities, incorrect mapping in the plasma core and/or plasma edge is present like discussed before.

6. Conclusions

A model for the ECE spectrum, realized by the ECE-raytracing code SPECE, and for the Michelson interferometer diagnostic, absolutely calibrated, at JET has been implemented into the framework Minerva. Besides the temperature profile, as provided by the standard analysis, the electron density and a correction for the vacuum toroidal magnetic field have been derived simultaneously and independently on other diagnostics. Therefore, the presented approach opens up the possibility for a fully self-consistent analysis. Several improvements with respect to the standard analysis have been achieved. Information about the plasma parameters is extracted from optically thick and thin regions of the ECE spectrum from 68-363GHz, i.e. several harmonics. The inferred temperature profile vanishes at the edge meaning that the pedestal becomes identifiable. Information about the density is extractable. Further improvements for the density and temperature profile are expected for a more detailed analysis including the profile uncertainties, the inference of $\psi_N(R,Z)$ and reflection and mode-scrambling coefficients of the in-vessel wall. The JET ECE diagnostic model of Minerva will be completed by adding the heterodyne radiometer with high time resolution [2]. By the high spectral resolution of the radiometer the shine-through region can be investigated to further improve the characterisation of the pedestal for both density and temperature.

References

[1] D.H. Martin and E. Puplett, Infrared Phys. 10, 105 (1969),
[2] E. de la Luna1, J. Sánchez1, V. Tribaldos,s et.al., Rev. Sci. Instrum. 75, 3831 (2004)
[3] J. Svensson and A. Werner, Proc. IEEE WISP (2007),
[4] S. Schmuck, H. J. Hartfuss, M. Hirsch., Proc. of the 36th EPS Conference on Plasma Phys. Sofia, Bulgaria (2009)
[5] D. Farina, L. Figini, P. Platania, and C. Sozzi, AIP Conf. Proc. 988, 128 (2008)
[6] L. Barrera1, Plasma Phys. Control. Fusion 52, 085010 (2010), [7] L. Figini et al., Rev. Sci. Instrum. 81, 10D937 (2010)
[8] J. Svensson, A. Werner, Plasma Phys. Control. Fusion 50 No 8, (August 2008)
[9] O. Ford, J. Svensson, A. Boboc, D. C. McDonald, Rev. Sci. Instrum. 79 (2008)
[10] O. Ford, J. Svensson, M. Beurskens, A. Boboc, J. Flanagan, M. Kempenaars, D. C. McDonald, E. R. Solano, EPS 2009, Sofia
[11] J. Svensson, et. al., Contributions to Plasma Physics 2, p 152-157, (3/2011)
[12] O. Ford, Tokamak Plasma Analysis through Bayesian Diagnostic Modelling, PhD thesis, Imperial College, London, 2010
[13] M. Hole, G. von Nessi, D. Pretty, J. Howard, B. Blackwell, J. Svensson, and L. Appel, Rev. Sci. Instr. 81, issue 10 (2010)
[14] M. Hole, G. von Nessi, M. Fitzgerald, K. G. McClements, J. Svensson, Plasma Phys. Contr. Fusion 53, 074021 (2011)
[15] S. Davis, M. Abrams, J. Brault, Fourier Transform Spectroscopy, ACADEMIC PRESS (2001), ISBN-10: 0-12-042510-6